Hindawi
Geofluids
Volume 2022, Article ID 5308530, 16 pages
https://doi.org/10.1155/2022/5308530

Research Article

Stability Control of a Roadway Surrounding Rock during the Cutting and Pressure Relief of a Coal-Bearing Roof at a Shallow Mining Depth

Chen Tian,[1,2] Yingjie Liu ,[3] Hezhuang Lou,[4] and Tinggui Jia[5]

[1]*Safety Engineering College, Heilongjiang University of Science and Technology, Harbin 150022, China*
[2]*CHN Energy Shendong Coal Group Corporation Ltd, Daliuta 719315, China*
[3]*Emergency Science Research Academy, China Coal Research Institute, China Coal Technology & Engineering Group Co., Ltd., Taiyuan 100013, China*
[4]*The No. 4 Pipe Network Operation Branch, Beijing Drainage Group Co., Ltd., Beijing 100044, China*
[5]*Inner Mongolia University of Science and Technology, Baotou 014000, China*

Correspondence should be addressed to Yingjie Liu; 290783585@qq.com

Received 29 July 2021; Revised 23 December 2021; Accepted 24 January 2022; Published 9 March 2022

Academic Editor: Jia Lin

Recent years have seen the widespread use of a new gob-side entry retaining technology, namely, automatic roadway forming based on roof cutting and pressure relief. However, because of the complex geological conditions, stability control methods for the surrounding rock remain unexplored. In this paper, through theoretical analysis, field measurement, and numerical simulation, the stability control of a roadway surrounding rock under roof-cutting and pressure-relief conditions is studied. The key stage in the steady-state control of this type of rock is determined by establishing a mechanical model of the hard roof in the process of automatic roadway formation. The results show that the roof-cutting and pressure-relief technology outperforms the conventional mining technology in terms of surface crack development and subsidence. The roadway roof movement can be divided into three stages: a direct roof-caving activity period, a basic roof-breaking activity period, and a roof-stabilizing period. The stress above the original roadway is gradually transferred to the adjacent working face, and a stress concentration is formed on the working face 6 m away from the roadway retaining section. In this scenario, the roadway is in a stress-reducing area, which ensures its safety. Based on the research results, we suggest adding a constant resistance and large deformation anchor cable near the cutting seam side for active support. A single-hydraulic prop + I-beam + steel mesh can support the working face, and a grouting bolt support can help reinforce the broken and loose surrounding rocks at the gangue-retaining side of the roadway. Thus, the movement of the surrounding rock can be effectively controlled. An industrial test shows that the effect of retaining roadway is evidently improved.

1. Introduction

Through nearly 60 years of exploration and practice, the gob-side entry retaining (GER) technology has achieved good results in applications, is now a relatively complete coal-pillar-free mining technology [1–5], and has promoted the development of coal-pillar-free mining. However, more attention should be paid to the stress concentration of the filling body and the poor matching between filling material and roof.

In the study of GER supports, various safety factors, support principles, and support methods have been proposed depending on the geological conditions through theoretical derivation, physical simulation, numerical simulation, and field monitoring [6, 7]. Through a computer simulation analysis of a roadway bolt support design, a sensitivity analysis method for the roadway support safety factor has been proposed [8,9]. The bolt strength, bolt shotcrete thickness, and lithology significantly influence the GER effect [10]. A constitution model was analyzed using linear elasticity, nonlinear elastoplastic, and elastoplastic theories. The post deformation and failure behavior of the rock mass has an important impact on the displacement and stress distribution of roadway surrounding

rocks. With the analysis results of a bolt support experiment [11], corresponding support countermeasures have been proposed [12, 13]. In the GER approach, the roadway-side support controls the basic roof of the roadway, and the control of the roof inclination serves as a theoretical basis for designing the working resistance and shrinkage of the roadside support [14, 15]. The roof activity law in different periods has a varying influence on retaining the roadway, and the mechanism of roadway-side reinforcement support can be explained through mechanical derivation. Accordingly, a roadway-side support principle has been proposed [16–19]. The interaction angle between roof movement and roadway-side support under mining action has a certain influence on the strength of the filling body for roadway protection, and the corresponding theoretical calculation method has been proposed [20, 21]. In recent years, the "soft rock large deformation theory" coupling support principle has been applied to fully mobilize the strength of deep stable rock strata and realize support integration and load uniformity. The theory has been verified by conducting several field experiments [22–25].

Significant research has been made on the behavior law of underground pressure distribution during GER. Studies have shown that rocks surrounding a roadway move violently because of the primary weighting and periodic weighting of the basic roof, resulting in support deformation, damage to GER roadway, and roof cracks or broken rocks [26–28]. The violent deformation of the roadway has a synchronous effect with the mining face weighting [29], and the roof subsidence increases in direct proportion with the increase in the roadway width and the hanging roof distance [30]. With the increase in the cutting height of the roadway-side support body with a high resistance along the GER section, the height of the roadway-side support of the caving rock increases. The roadside support body and surrounding rock can be made to reach a new balanced state as soon as possible by fully utilizing the bearing capacity of the caving gangue, thereby reducing roadway deformation [31, 32]. Moreover, a GER support cannot easily prevent any changes in the upper stratum balance. Nevertheless, a sufficient support resistance can help avoid serious fractures on the direct roof, prevent the formation of a large separation layer between the upper layers, and directly realize basic roof cutting at the goaf side [33]. Therefore, improving the support strength has a positive effect on controlling the surrounding rock for retaining roadways [34–36].

Automatic roadway formation through roof cutting and pressure relief is a new pillar-free mining technology [37,38]. In this approach, the stress transfer of the overlying strata is cut off via bidirectional energy accumulation blasting at the cutting seam [39], and the roof rock mass collapses to form a roadway side, thus realizing an automatic roadway formation in working face mining. Self-formed roadways without coal pillars have been realized through the roof cutting and pressure relief of medium-thick coal seams [40–42]. Results have shown that the stress condition of roadway surrounding rocks during this process can be improved, and a support technology has been established to adapt to the deformation of roadway surrounding rocks and to control their stability. Currently, there is little research on the stability control of the surrounding rocks of shallow-buried and deep-coal-bearing composite roadways under roof-cutting and pressure-relief conditions. Moreover, research on roof-cutting and pressure-relief technology under the condition of a shallow coal seam hard roof is insufficient.

Therefore, based on the rock mechanics during roof cutting and pressure relief, this study establishes a mechanical model of a hard roof in the process of roof cutting and pressure relief, analyzes the key stages in the stable control of a roadway, and obtains the surrounding of shallow-buried and deep-coal-bearing roadways. Finally, field verification was carried out to validate the results.

2. Geological Conditions of the 12201 Working Face

The 12201 fully mechanized face of Halagou Coal Mine was the first working face of the second panel of a coal mine 12#, with an inclined face 320 m in width and 747 m in length (from the cutting hole to the stopping line). The GER section was 580 m in length. As for the face, the coal seam thickness ranged from 0.8 m to 2.2 m. The average mining height was 2 m. The workable reserve reaches 61 Mt. The coal seam was relatively stable, with the 12202 face on the northwest, which was the only face nearby. Figure 1 shows the layout of the 12201 fully mechanized face.

In terms of the lithology of this face, the thickness of the overlying bedrock ranged from 55 m to 70 m, whereas the thickness and depth ranges of the unconsolidated layers were 0–33.48 m and 60–100 m, respectively. The immediate roof of the coal seam was composed of siltstone, which had an average thickness of 1.84 m. The No. 12 upper coal seam was laid above the immediate roof, and its average thickness was 1.56 m. The top of the coal seam contains mudstone with an average thickness of 1.35 m. The main roof of the coal seam was made of fine-sandstone and siltstone; the average thicknesses of which were 3.34 m and 4.05 m, respectively. The immediate floor of the face was made of siltstone with an average thickness of 3.67 m. At the bottom of the immediate floor was fine-sandstone with an average thickness of 4.23 m. Figure 2 shows the lithology of the 12201 fully mechanized face.

3. RCPR Gob-Side Entry Retaining Parameter Design

An adequate height is required for roof cutting to ensure that the movement of the rock beam on the main roof of the overlying strata in the goaf is supported by the caving gangue. Based on previous research and based on the analysis of key parameters of automatic roadway with RCPR, the influence of height and angle of roof cutting on the strata behaviors had been simulated and studied with the FLAC^{3D} numerical simulation software, which confirmed that the optimal roof cutting height and splitting angle of the 12201 working face of Halagou Coal mine were 6 m, respectively. The effect of automatic roadway with RCPR had been well implemented through conducting the bidirectional

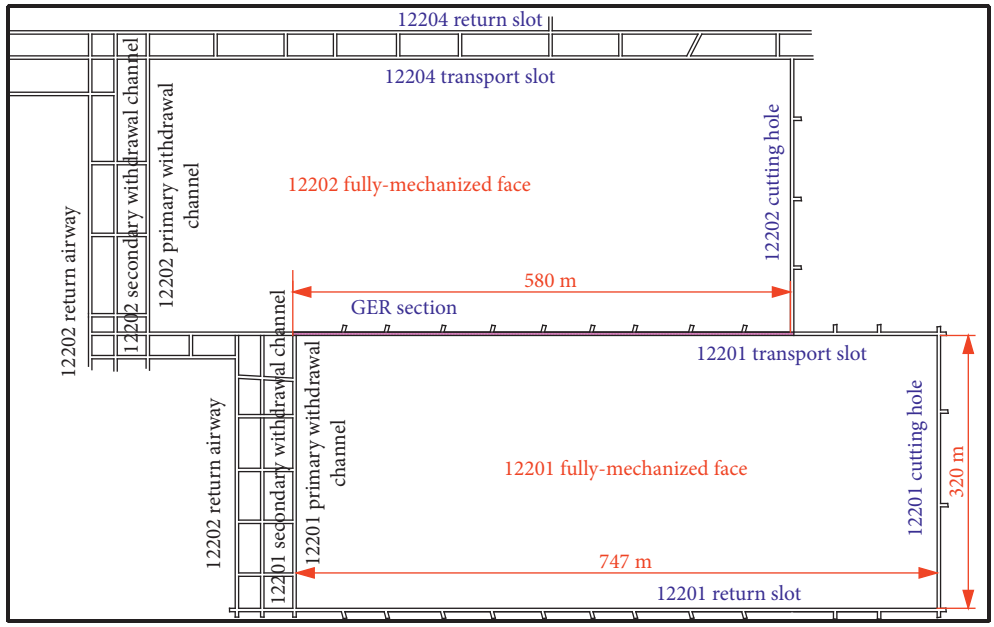

Figure 1: Diagram of the 12201 work surface layout.

Stratum	No.	Depth of stratum/ m	Histogram	Rock name
Yan'an group	1	4.63~0.03 / 4.05		Siltstone
	2	4.18~2.50 / 3.34		Fine sandstone
	3	2.14~0.55 / 1.35		Mudstone
	4	2.75~0.00 / 1.56		No. 12 uppercoal
	5	3.90~0.52 / 1.84		Siltstone
	6	2.30~0.80 / 1.92		No. 12 coal
	7	10.40~0.15 / 3.67		Siltstone
	8	7.75~2.40 / 4.23		Fine sandstone

Figure 2: Comprehensive histogram of the 12201 fully mechanized mining face.

cumulative blasting test on-site [43–45]. The height could be determined using the following equation:

$$H_m = \frac{(H_{coal} - \Delta H_1 - \Delta H_2)}{0.3}. \quad (1)$$

Since the coal seam of the 12201 fully mechanized face had a composite roof, the roof-cutting height was set as 6 m. Considering the significant angle effect on the fracture, the cutting angle should be measured carefully to optimize the roof caving in the goaf and realize a reasonable stress distribution by adjusting the stress concentration area. In the present study, the cutting angle was set to 20° [46].

The bilateral cumulative tensile explosion was employed for directional roof cutting. In this approach, two shaped charges were placed in a gathering device with two preset blasting directions. After detonation, pressure from directions other than the preset ones was uniformly applied to the surrounding rock around the blasting boreholes, which were in tension in the preset directions simultaneously. In this study, the optimal charge quantity was set as 3 + 2+0 + 1. The distance between the boreholes was 0.6 m. The thickness of the boreholes was 6.0 m. The optimal luting length was 0.5 m. Ten boreholes were generated in each explosion. Figure 3 shows the borehole layout [47].

4. Ground Pressure Behavior Law of Roof-Cutting and Pressure-Relief Stope with Three Shallow-Buried Composite Roofs

4.1. Analysis of the Ground Pressure Behavior Law in Stope Area. The stope was mainly divided into three stratum pressure areas: a roof-cutting influence area, a nonaffected area in the middle, and a noncutting area, as shown in Figure 4.

Based on the division of the roadway under roof unloading, seven hydraulic supports, denoted by 5#, 10#, 20#, 90#, 100#, 125#, and 165#, were selected for ore-pressure monitoring, among which 5#, 10#, and 20# were located in the affected area of the roadway under roof unloading, 90# and 100# were located in the middle unaffected area, and 125# and 165# were located in the unroofed area. Figure 5 shows the pillar loads in the areas affected by roof cutting, pressure relief, and roadway retention.

4.1.1. Periodic Pressure Step Distance. The supports 5#, 10#, and 20# were in the conventional coal mining process area at the beginning of the mining stage of the working face. When

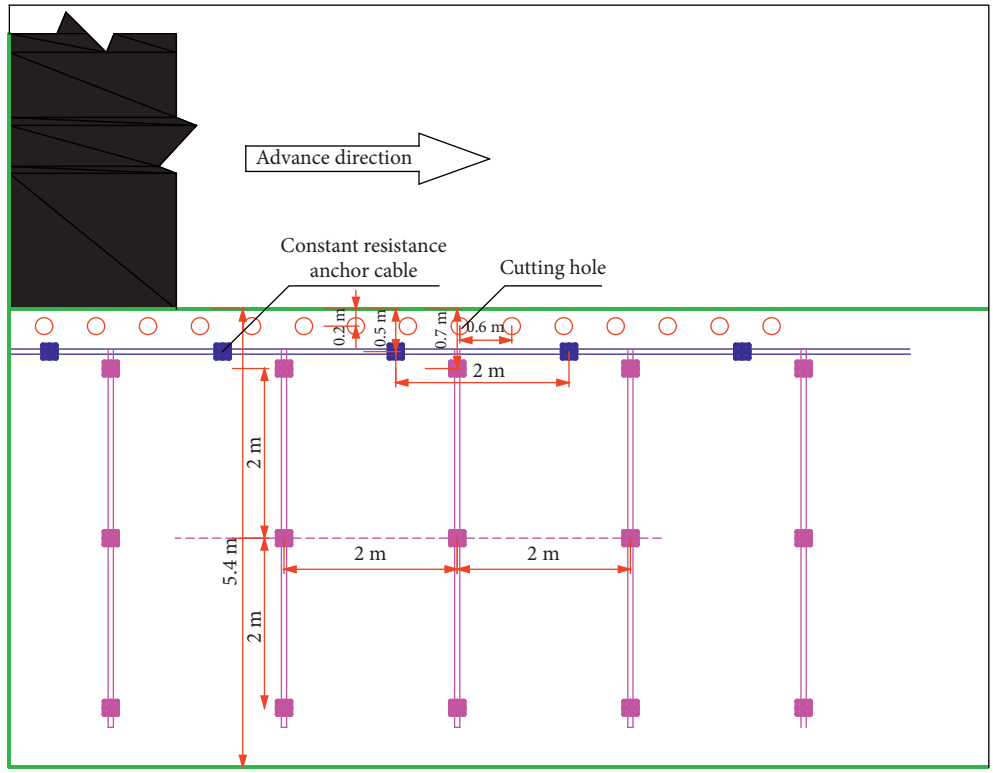

Figure 3: Slot hole layout plan.

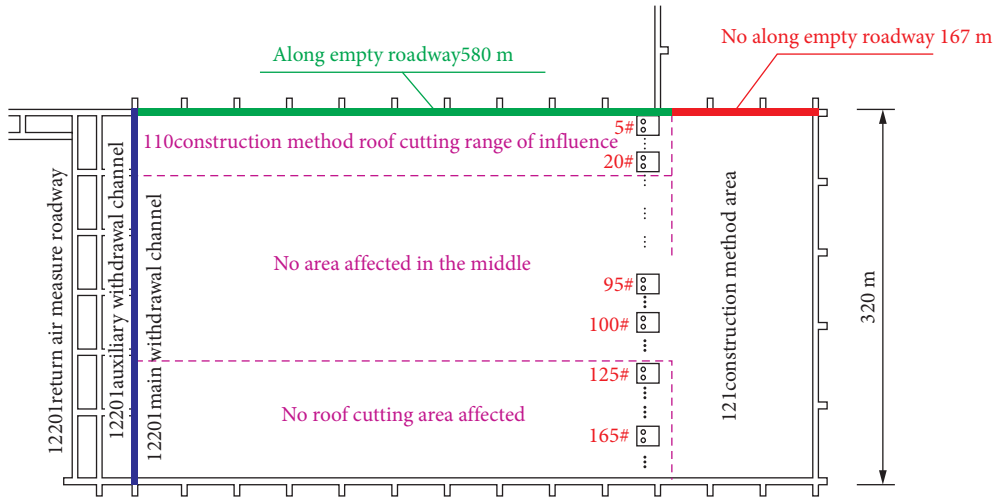

Figure 4: Division of the roof-cutting and pressure-relief roadway retaining project.

pushed to 173 m, the three supports enter the influence areas of roof cutting, pressure relief, and roadway retention. Table 1 lists the periodic pressure step distances of the 5#, 10#, and 20# brackets in the above two stages.

Compared with the conventional coal mining process area, the periodic pressure step distance in the area affected by the cutting of the roof unloading and retaining roadway increases by a range of 18–22 m, i.e., by approximately twofold. The periodic pressure step increased under the influence of roof cutting pressure relief shows large direct jacking height and small lumpiness at the end of the working face (large coefficient of breaking expansion), the filling effect of goaf was good, the gangue formed into a burst could usually fill the goaf, and the base roof had less room for rotation. The smaller the rotation angle, the smaller the rotary deformation. As a result, the basic roof was not easy to break; the fracturing step was increased.

4.1.2. Support Resistance. In the process of advancing with the stope, the three supports passed through the conventional coal mining process area and the cutting roof

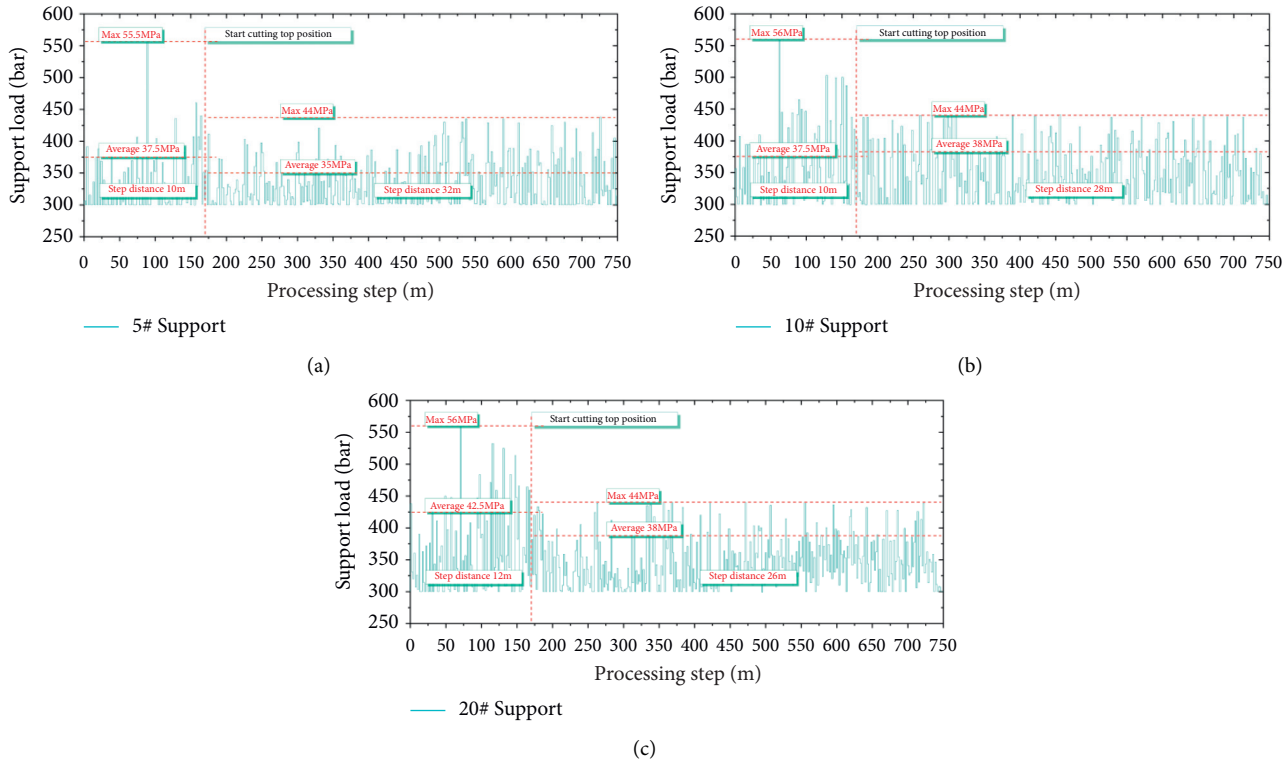

Figure 5: Load curves of support pillars in areas affected by roof cutting in the roof-unloading, retaining roadway: (a) No. 5, (b) No. 10, and (c) No. 20.

Table 1: Pressure cycle steps and pressure in areas affected by roof cutting in the roadway.

Hydraulic support	Conventional coal mining area (m)	Influence areas of cutting roof reserved for cutting-roof pressure relief (m)
No. 5	10	32
No. 10	10	28
No. 20	12	33

influenced areas of the roof unloading and retaining roadway. Table 2 provides the load statistics of the supports in the two stages.

The chart shows that, compared with the conventional coal mining process, the maximum pressure during the periods of roof cutting, pressure relief, and roadway retention was reduced by a range of 10–12 MPa or by approximately 20%. The basic roof fracture interval increased. However, the support working resistance decreased. The fracture step of the basic tip increased, but the working resistance of the support decreased. It showed that when the direct roof breaks down and falls behind, the broken and swollen gangue could basically fill the goaf under the influence of cutting head blasting. The base roof had less room to rotate. Therefore, the rotary deformation was also small, and the direct roof of the goaf retention lane was also small.

4.1.3. Unaffected Area and Uncut Top Area in the Middle. Figure 6 shows the load curves of the 95#, 100#, 125#, and 165# supports.

The maximum and average periodic pressures of the support in the middle of the working face were 60 and 44 MPa, and the step distance of the periodic pressure was in the range of 10–20 m. The maximum periodic pressure was 55 MPa, and the average value was 37 MPa. The step distance of the periodic pressure was in the range of 8–12 m. Based on the load curves of the support pillars in the middle unaffected area (95#, 100#) and uncut top area (125#, 165#), the values of the periodic pressure step and the support load are listed in Table 3.

4.2. Analysis of the Variation Law of Force Expansion and Contraction of the Anchor Cable with Constant Resistance and Large Deformation. Based on the advance of the working face and the arrangement of the anchor cable stress meter, we selected stress monitoring points 11# and 12# on the anchor cable, located 331 m away from the open-cut hole of the 12201 working face.

The analysis shows the following:

(1) The advance concentrated stress generated by the advance of the working face had an impact on the stress of the anchor cable, and the advance influence range was generally up to 30 m, such as at the measuring points 15#, 14#, and 13#

Table 2: Support load (MPa) in areas affected by roof cutting in the roof-unloading and retaining roadway.

Hydraulic support	Conventional coal mining area			Influence area of cutting roof is reserved for cutting-roof pressure relief		
	Maximum	Minimum	Average	Maximum	Minimum	Average
No. 5	55.5	33	37.5	44	32	35
No. 10	56	31	37.5	44	30	38
No. 20	56	35	42.5	44	32	37.5

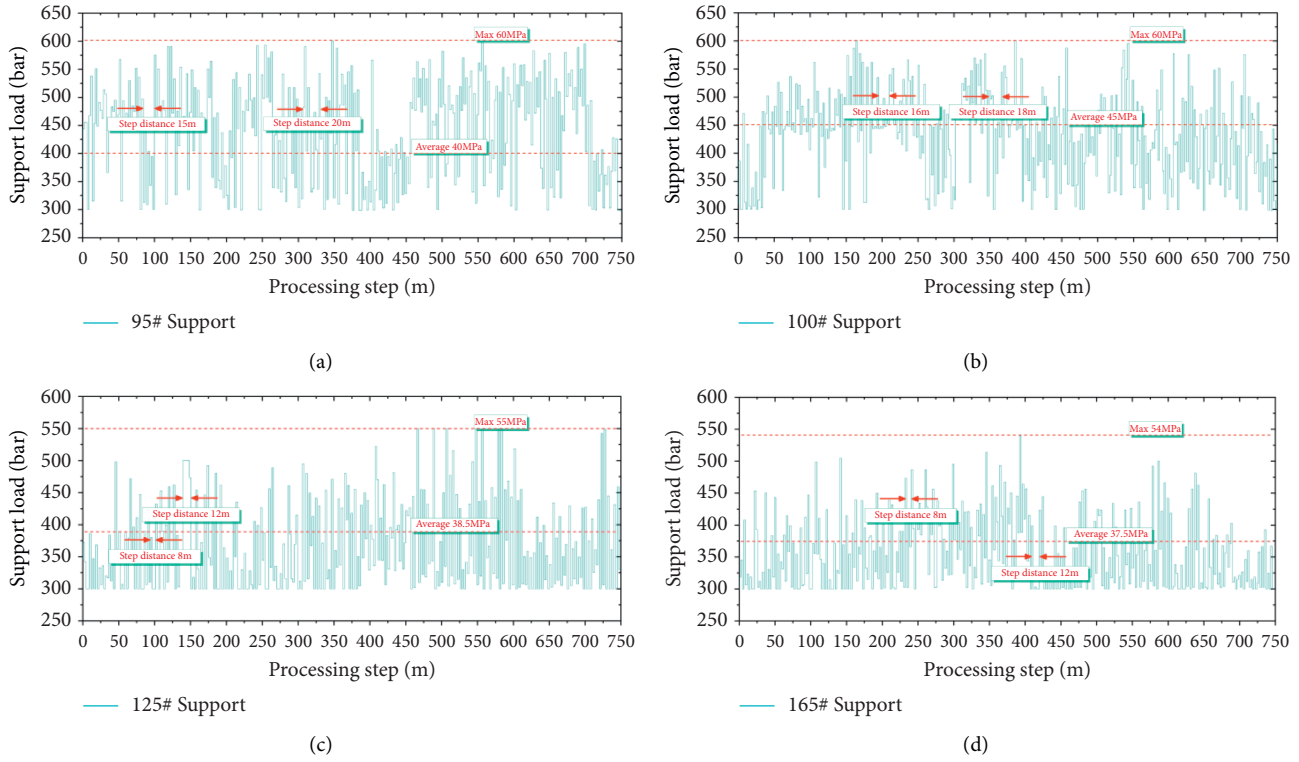

Figure 6: Pillar load curves of supports in the middle unaffected area and uncut top area: (a) No. 95, (b) No. 100, (c) No. 125, and (d) No. 165.

Table 3: Support load and periodic pressure step in the middle of the unaffected area and uncut top area.

Area	Hydraulic support	Hydraulic support load (MPa)			Periodic pressure step (m)
		Maximum	Minimum	Average	
Middle unaffected area	No. 95	60	32.5	44.2	10–20
	No. 100	60	34	45	10–20
Uncut top area	No. 125	55	32	38.5	8–12
	No. 165	54	31.5	37.5	8–12

(2) When the strike length of the goaf was equal to the trend length, the stress was concentrated, there was evident ore-pressure formation, the deformation of the roof and floor was large, and roof caving occurs easily

When the working face was pushed 319 m, a large stress concentration occurred, leading to an increase in the anchor stress value at the measuring points 11# and 12# in front of the working face. Figure 7 shows the change curve of the anchor stress value.

Table 4 presents the key position and maximum tensile stress on the stress curve of the anchor cable.

4.3. Analysis of the Variation Law of Roof Separation. Based on the advance of the working face and the arrangement of the roof separator, five monitoring points 1#, 2#, 4#, 5#, and 6# were selected, positioned 260, 280, 330, 430, and 480 m away from the open-cut eye of 12201 working face.

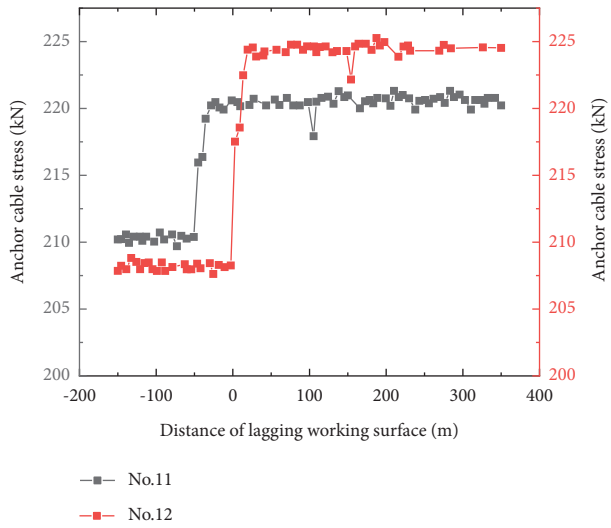

Figure 7: Variation curve of anchor cable stress obtained using a stress meter.

Table 4: Key positions and maximum tensile stress of the anchor cable stress change curve.

Anchor cable stress monitoring point	Distance from opening to 12201 sides (m)	Curve increases its starting position (lag face distance) (m)	Maximum tensile stress of the anchor cable (kN)
No. 15	241	−31	124.1
No. 14	261	−26	232.6
No. 13	281	−41	286.7
No. 12	331	−13 (fully mechanized face stopped to 319 m)	225.2
No. 11	381	−63 (fully mechanized face stopped to 319 m)	221.3

The analysis shows the following:

(1) The advance of the working face had an impact on the roof separation of the roadway, which was generally within ±50 m. When the roadway roof condition was poor, it was mainly affected by the advance concentrated stress of the working face, such as at measuring points 1# and 2#. When the roadway roof condition was good, it is mainly affected by the stress of the short-wall beam formed after mining, such as at measuring points 5# and 6#.

(2) Based on the stable position of the curve at the monitoring points 4, 5, and 6, after the stoping of the working face, when the roof separation value tended to stabilize, the distances of the lagging working face were 81, 81, and 94 m, respectively.

In other words, when the distance of the lagging working face was greater than 95 m, the roadway roof separation tended to be stable. Figure 8 shows the variation curve of the roof separation value at the roof separation monitoring point. Table 5 shows the key position and maximum value of the roof separation change curve.

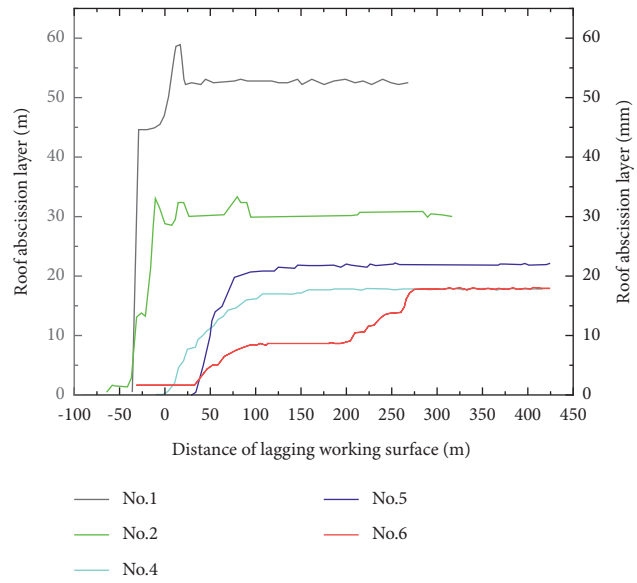

Figure 8: Variation curve of roof separation.

4.4. Analysis of the Variation Laws of the Abutment Pressure and Shrinkage under Lagging Single Pillar. Four monitoring points for the supporting pressure and shrinkage under lagging single pillars (2#, 7#, 12#, and 13#) were selected, located 26, 73, 176, and 205 m away from the open-cut hole of the 12202 working face, respectively.

The analysis shows the following. (1) The abutment pressure of the lagging single pillar was mainly manifested in two ways. ① It quickly reaches the rated support force and

Table 5: Key positions and maximum value on the roof separation variation curve.

Roof separation monitoring point	Distance from opening to 12201 sides (m)	Curve increases its starting position (lag face distance) (m)	Curve starts at a smooth position (lag face distance) (m)	Maximum ceiling separation (mm)
No. 6	260	33	81	17.9
No. 5	280	31	82	22.0
No. 4	330	−2	94	17.8
No. 2	430	−48	8	33.4
No. 1	480	−34	−29	58.4

fluctuates in a certain range, such as at the pillar measurement points 7 and 12. ② After the working surface advances a certain distance, it gradually reached the rated support force and fluctuates within a certain range, such as at 2# and 13# pillar measuring points.

(2) From the stable position of the curve at the monitoring points 2, 7, 12, and 13, we found that after the stoping of the working face, when the maximum shrinkage under the active column tended to be stable, the distances of the lagging working face were 90, 92, 98, and 102 m, respectively.

When the distance of the hysteresis working face was greater than 100 m, the subsidence of the roadway roof tends to stabilize. This was consistent with the previous conclusion that "roadway roof separation tended to be stable only when the hysteresis working face distance was greater than 95 m."

Figure 9 shows the curves of the abutment pressure and shrinkage under the active columns at the monitoring points on the single pillar. Table 6 shows the key positions and maximum value of the accumulated shrinkage of the active columns.

4.5. Analysis of the Variation Law of Roadway Lateral Pressure. Two side-pressure monitoring points were arranged at the side of the goaf of the roadway, 240 m and 302 m away from the open-cut hole of the 12202 working face. The maximum lateral pressure value at the monitoring point 1# is 2.0 MPa, and the average value was 1.7 MPa after stabilization, i.e., 30 m behind the working face. The maximum lateral pressure value at the monitoring point 2# is 0.8 MPa, and the average was 0.7 MPa after stabilization, i.e., 39 m from the lagging working face. Figure 10 shows the monitored lateral pressure values and their variation curves at the two lateral pressure monitoring points.

4.6. Comparative Analysis of Surface Deformation. A field observation showed that the surface deformation of the roof-cutting and the pressure-relief-retaining roadway was significantly lower than that under the conventional long-wall mining condition. The crack width was small, in the range of 1–3 mm. Table 7 compares the surface subsidence and damage. Figures 11 and 12 show a comparison of the surface fracture development zones and actual conditions.

Based on the above analysis, the roof movement along the goaf roadway could be divided into three stages: an active stage of direct roof caving, an active stage of basic roof breaking, and a stable roof stage.

4.6.1. Direct Jacking Falls Active Period. With the advance of the working face, the support constantly moved forward, and the roof strata at the rear of the working face lost support from the supports. The direct roof of the goaf side of the retention lane was under the action of cutting force generated by dead weight. The edge of the backfill near the direct roof roadway was broken. It is like an upside-down step in the state of the cantilever beam. At this stage, under the drive of the direct roof caving and the basic roof sinking, the deformation of the goaf roadway roof was mainly rotational deformation. The roof activity in this stage also was the direct roof-caving activity period. When the direct roof collapse could fill the goaf, the basic roof strata break and collapse. The basic roof could form a masonry structure to achieve stability in the balance process.

4.6.2. Active Period of Basic Roof Rupture. When the direct roof strata were not enough to fill the goat, the basic roof strata would also collapse the flexure fracture, filling goaf forms masonry structure, and in the process of motion balance, because the stiffness of the coal body was greater than that of caved gangue in goaf. Therefore, the weight of the overburden on the basic roof was gradually transferred to the depth of the coal beside the roadway through the direct roof; stress concentration occurred in the deep part of the coal body and rotates with the basic roof block. The basic roof rock gradually stabilized under the support of falling gangue at the bottom, so that the surrounding rock stress along the goaf was lower than the original rock stress.

4.6.3. Roof Stabilization Period. The deformation is still largely driven by rotation, characterized by a high speed and magnitude. In this period, the deformation of the roof accounts for 60–70% of the total rotation-induced deformation of the roadway. With the gradual compaction of the gangue, the stable upper strata would also break, deform, and sink, thereby damaging the coal wall and even the direct roof. The abutment pressure range would increase, the peak value would continue to move inward, and the roof above the retaining roadway would sink in parallel. Because of the influence of the stratified collapse of the basic roof, the roof of the roadway would sink in a fluctuating manner. The roof movement was mainly parallel subsidence. However, the subsidence speed is low.

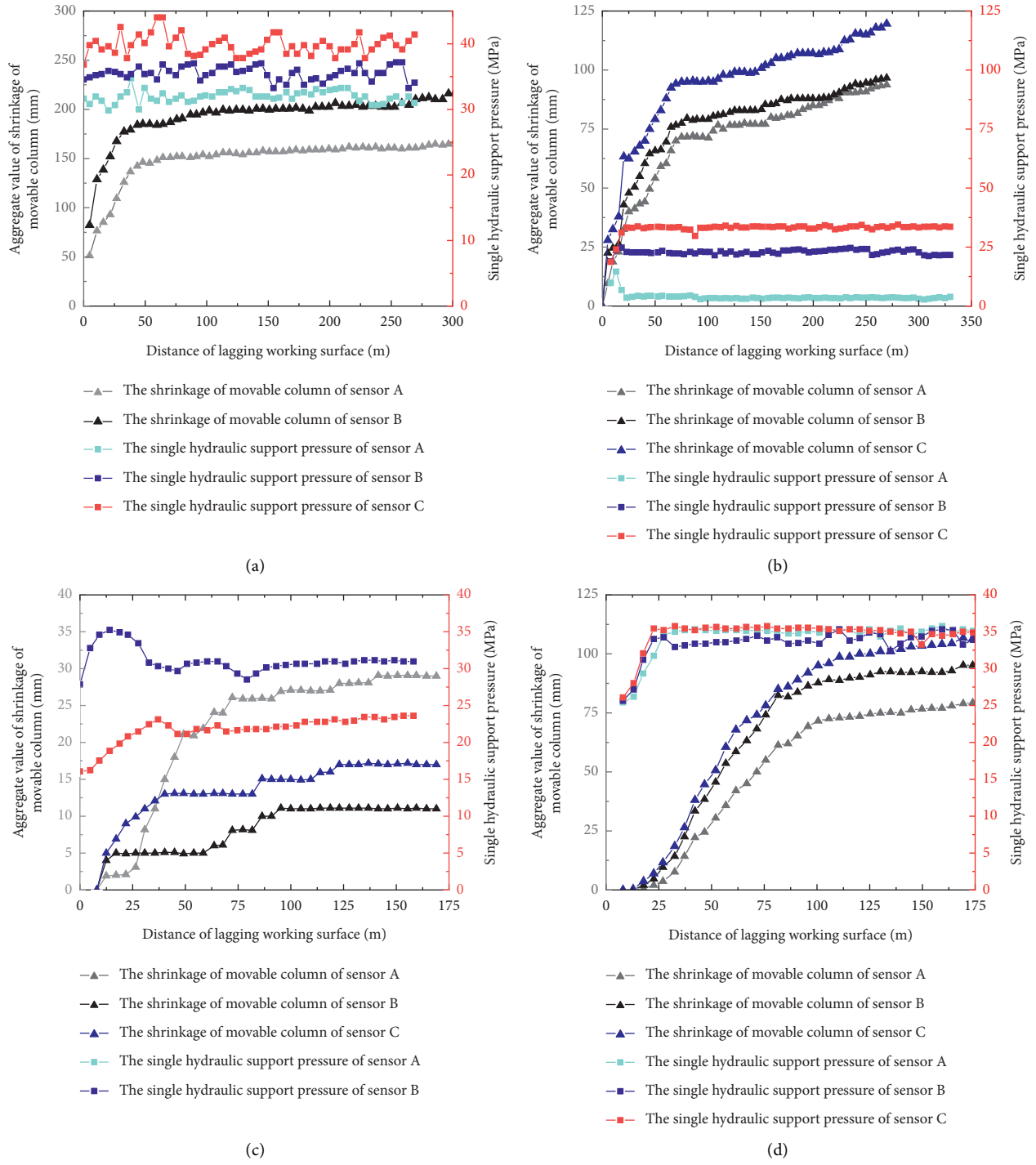

Figure 9: Data recorded at each monitoring point in the section along the hollow lane: (a) No. 2, (b) No. 7, (c) No. 12, and (d) No. 13.

5. Numerical Simulation of Mine Pressure Development in Shallow-Buried, Composite Roof-Cutting, Unloading Stope

To better study the mining pressure distribution rules of the automatic roadway formation working face under roof-cutting and pressure-relief conditions without coal pillar mining, we should analyze the movement mode of the stope roof and upper rock strata, understand the movement mechanism and stress distribution of the surrounding rock more clearly, and effectively guide the selection of the support and corresponding equipment in the future.

Based on the actual situation on-site, a step-by-step numerical simulation of the mining process was carried out for a distance of 15 m each time, with the simulated stoping length being 60 m. The initial stresses imposed in the x-direction, y-direction, and z-direction are 10 MPa, 10 MPa,

Table 6: Key positions and maximum value of the accumulated lower shrinkage of active columns on the change curve.

Measure point	Curve starts at a smooth position (lag face distance) (m)	Maximum shrinkage under the active column (mm)
No. 2	92	217
No. 7	90	120
No. 12	98	29
No. 13	106	102

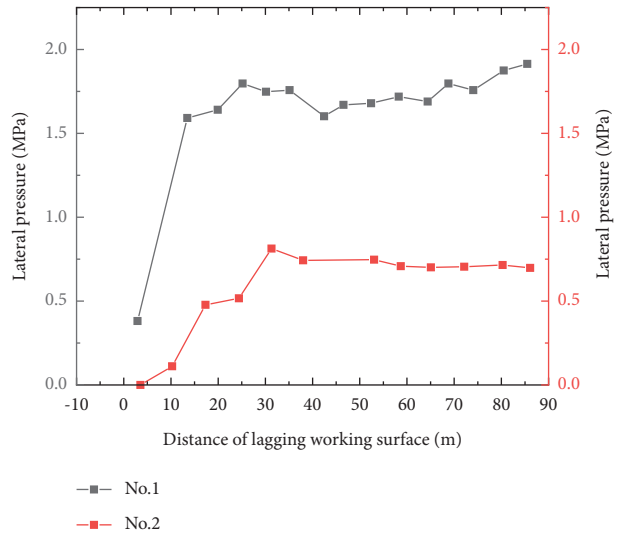

Figure 10: Variation curve of lateral pressure at the monitoring points.

Table 7: Comparison of surface subsidence and damage.

Classification	Cut off the roof pressure to leave the roadway area	Conventional coal mining area	Contrasting condition
Steps to sink (mm)	<5 mm	400–750 mm	Retaining roadway for roof-cutting pressure relief basically eliminate the step sinking
Crack width (mm)	1–3 mm	10–20 mm	Crack width reduction 75%
Crack interval (m)	30–40 m	8–10 m	Fracture density reduction 70%

and 15 MPa, respectively. The burial depth is set to 200 m. The working face width is 300 m.

As shown in Figure 13, when the working face was excavated for 15 m, the pressures on the tail and middle sides were relatively high. The vertical stress on the working face near the cutting seam alignment slot was 2.4 MPa and that on the end side was 3 MPa.

The horizontal stress on the working face close to the slotting groove was 0.9 MPa and that on the end side was 1.2 MPa. The pressure of the slotting groove was reduced by 25% compared with that on the end side.

As shown in Figure 14, after 30 m excavation of the working face, it experienced the initial pressure of the basic roof, and the initial pressure step distance was about 40 m. The overall pressure of the working face was small after the basic roof pressure at this time. The vertical stress of the working face close to the slotted groove was 2.09 MPa, the end side was 2.6 MPa, and the side pressure of the slotted groove was reduced by 20% compared with that of the end side. The horizontal stress on the working face close to the slotted groove was 1.092 MPa and that on the end side was 1.4 MPa. The pressure on the slotted groove side was 22% less than that on the end side.

As shown in Figure 15, after 45 m of excavation, the vertical stress of the working face near the slotting groove was 1.8 MPa, whereas that on the tail side was 3.0 MPa. The side pressure of the slotting groove was reduced by 40% compared with that at the end. The horizontal stress on the working face close to the slotting groove was 0.9 MPa and that on the end side was 1.2 MPa. The pressure on the slotting groove side was reduced by 25% compared with that on the end side.

As shown in Figure 16, after 60 m of excavation, the working face experienced a periodic pressure, and the pressure step distance was 30 m. The vertical stress on the working face close to the slotted groove is 2.6 MPa, whereas that on the tail side was 3.12 MPa. The pressure on the slotted groove side was reduced by 30% compared with that at the end. The horizontal stress on the working face close to the slotting groove was 0.9 MPa and that on the end side was

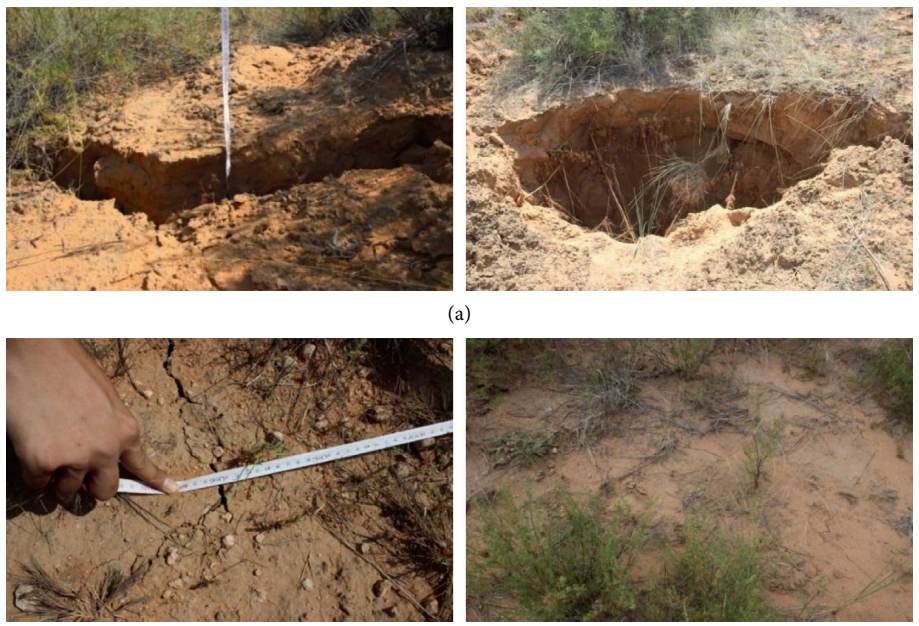

(a)

(b)

Figure 11: Comparison of surface fractures. (a) Surface fractures in the conventional coal mining process. (b) Surface cracks in the roadway retained by roof cutting and pressure relief.

Figure 12: Surface fracture development zone comparison.

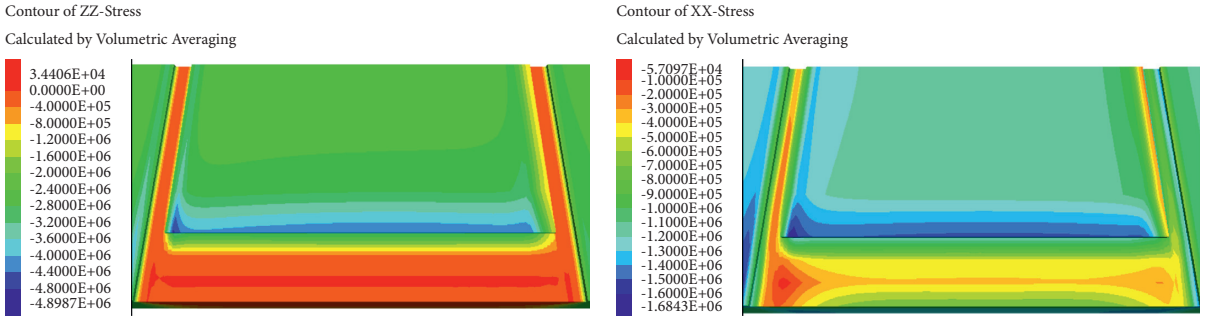

(a) (b)

Figure 13: Stress distributions while excavating a face for 15 m. (a) Vertical stress. (b) Horizontal stress.

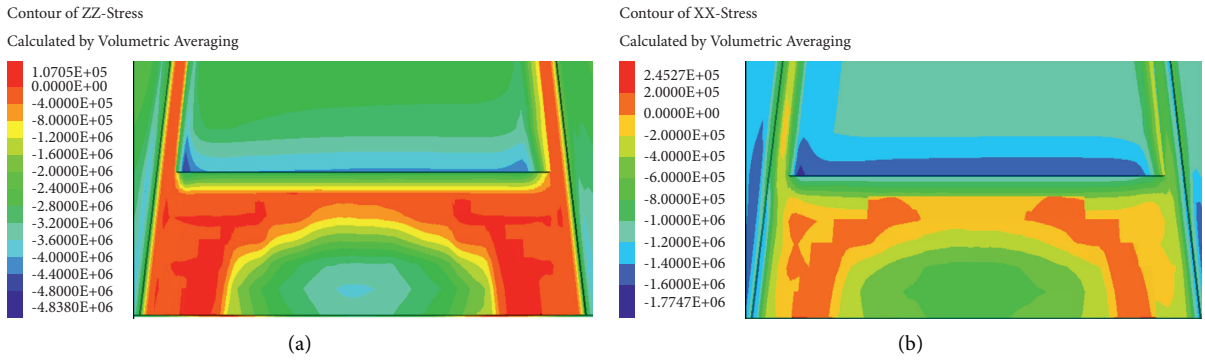

Figure 14: Stress distributions while excavating a face for 30 m. (a) Vertical stress. (b) Horizontal stress.

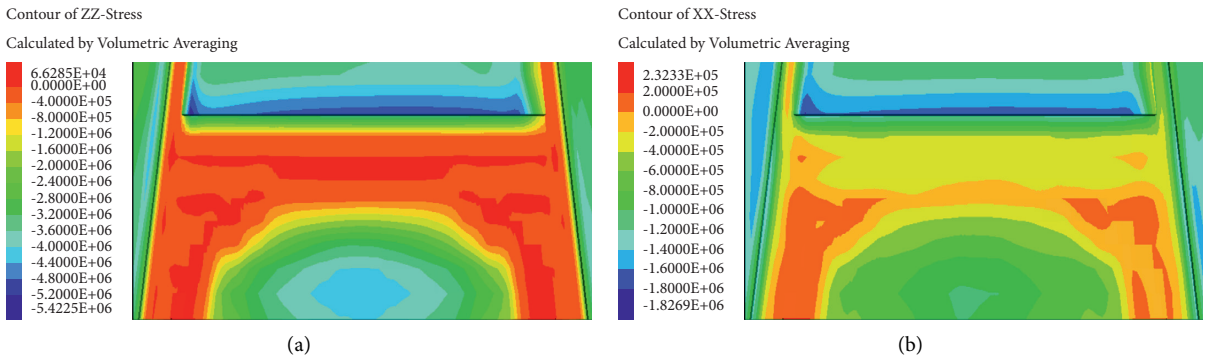

Figure 15: Stress distributions while excavating a face for 45 m. (a) Vertical stress. (b) Horizontal stress.

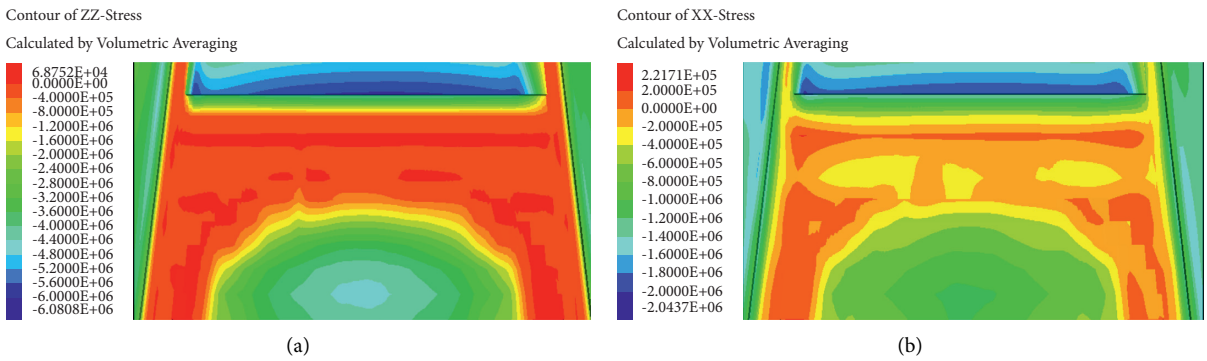

Figure 16: Stress distribution while excavating a face for 60 m. (a) Vertical stress. (b) Horizontal stress.

1.2 MPa. The pressure on the slotting groove side was reduced by 25% compared with that on the end side.

To sum up, in the cut after unloading without the coal pillar mining technology, the original stope stress distribution was changed, particularly on the cutting seam gateway side. After the mining face overburden formation of the cantilever beam structure, a protective space was formed along the trough; the safety of the tunnel was ensured. The original side pressure of the coal pillar along the trough was transferred to the depth of the adjacent working face. Moreover, the simulation results show that stress concentration was formed at 6 m away from the adjacent working face to the roadway, and the stress distribution of the original working face also changed.

By comparing the actual situation on-site with the numerical simulation, the following can be concluded:

(1) The pressure on the working face of the slotting side was low, the vertical stress was reduced by approximately 27.5%, and the horizontal stress was reduced by 24.25%. The same numerical simulation shows that the influence range of the roadway on the mining pressure of the working face was 25 m, consistent with the actual measured data on-site.

(2) The periodic pressure step of the working face was 30 m, and the actual on-site periodic pressure step was approximately 30 m, an increase of approximately 1 m compared with the original periodic pressure step.

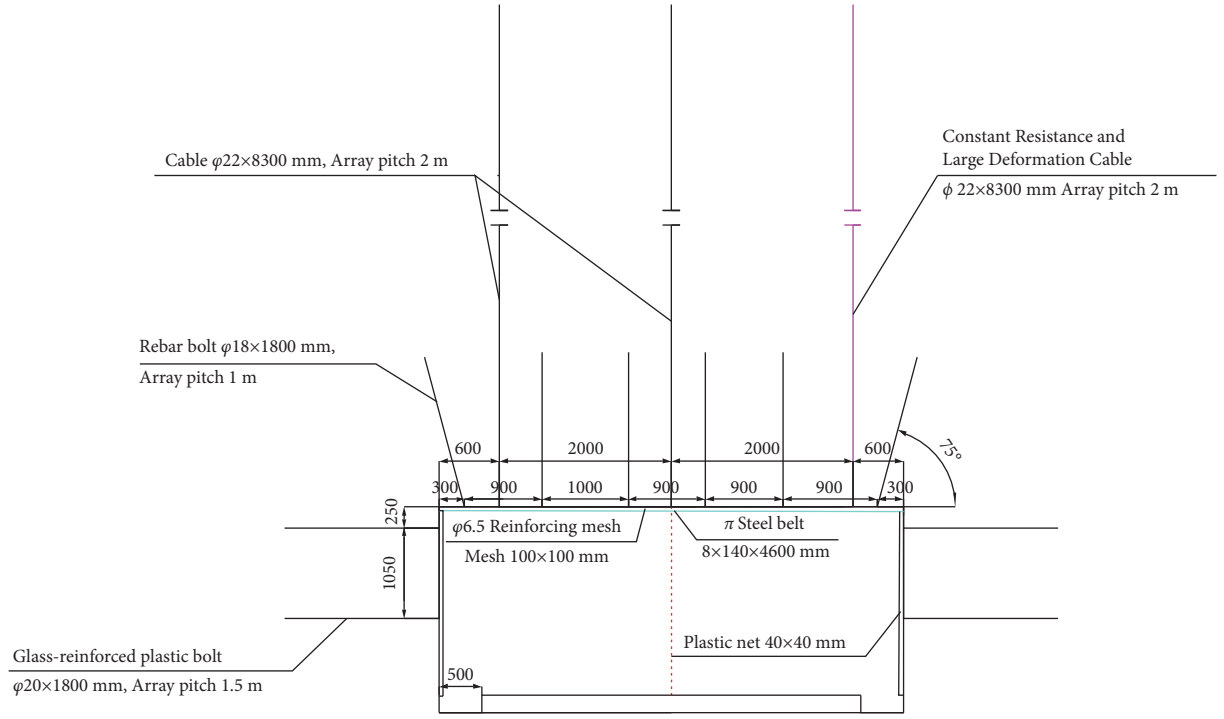

Figure 17: Design section of trough support.

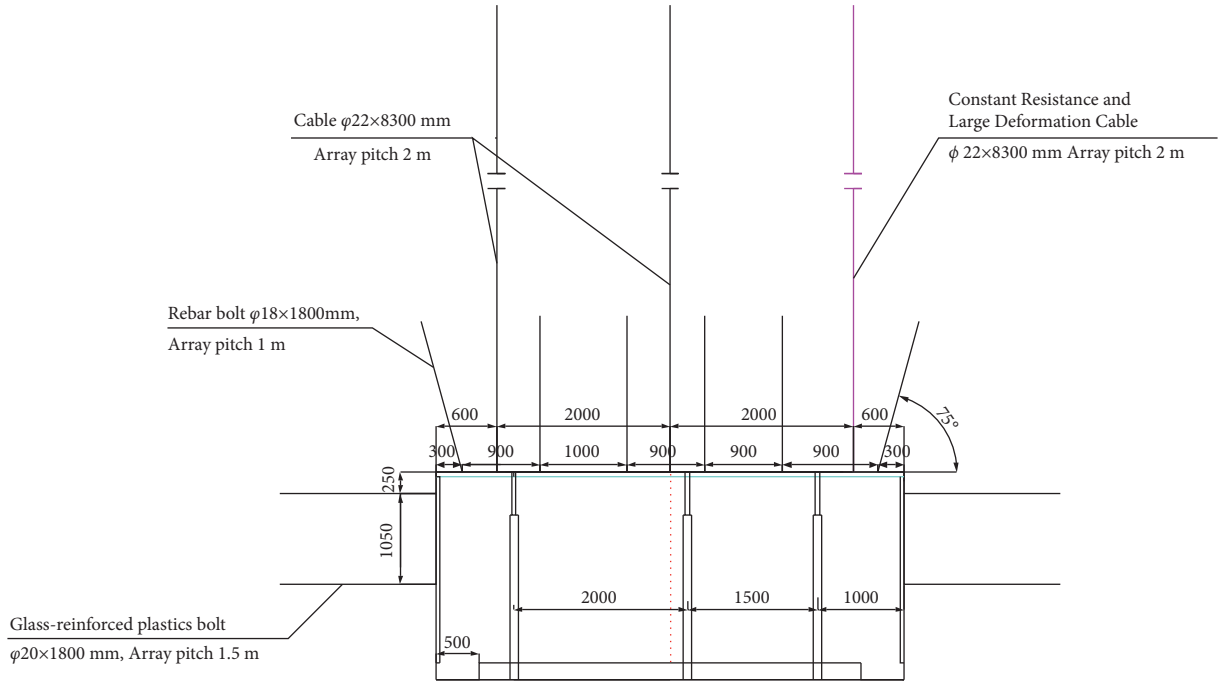

Figure 18: Sectional drawing of a single support in the lane.

(3) After the application of roof-cutting and pressure-relief technology, the stress above the original roadway was gradually transferred to the adjacent working face, forming a stress concentration inside the working face 6 m away from the retained roadway. Nevertheless, the retained roadway was in the stress-reduction zone, thus ensuring its safety.

6. Steady-State Control of the Surrounding Rock under Roof Pressure Relief

Based on the analysis results of field monitoring and numerical simulation, we optimized the relevant parameters of the coal-pillar-free mining technology for automatic roadway formation under the condition of a shallow-buried deep coal-bearing

(a) (b)

Figure 19: Effect diagram of the roadway (a) before and (b) after optimization.

composite roof, to avoid repeated investment on support. The specific optimization parameters are as follows.

6.1. Support Parameters of the Chute

① The roof is supported by an ordinary anchor cable and large deformation anchor cable with constant resistance. Make a row of anchor and large deformation along the roadway strike at the reserved slit side. Anchor rod adopts rebar bolt; anchor cable was connected with type steel belt and spread 6.5 rigid mesh in the roof rock face.

② The upper part used a 20 mm × 2000 mm fiberglass bolt, the spacing between the rows was 1050 mm × 1500 mm, and the plastic mesh grid is 40 mm × 40 mm.

③ Roof anchor cable (common anchor cable and constant resistance large deformation anchor) used 22 mm × 8300 mm steel strand, with the row spacing of 2000 × 2000. Among them, the distance between the constant resistance and large deformation anchor cable was 600 mm, the rebar anchor rod was 18 mm × 1800 mm, and the spacing between rows was 900 mm × 1000 mm. The rock bolt near the side of the side and the vertical line were arranged at an angle of 15°. The steel belt was 8 mm × 140 mm × 4600 mm, the steel mesh was 6.6 mm in diameter, and the mesh size was 100 mm × 100 mm. Figure 17 shows the optimized supporting section along the groove.

6.2. Single Support in the Roadway. Based on the analysis of the practical application on-site, the influence of supporting pressure on the roadway was reduced after roof cutting, pressure relief, and roadway retention. The supporting form of the roadway could be "one beam and three columns," as shown in Figure 18. Figure 19 shows the field application effect.

7. Conclusion

In this paper, through theoretical analysis, field measurement, and numerical simulation, the stability control of a roadway surrounding rock under roof-cutting and pressure-relief conditions is studied. The main conclusions are as follows.

(1) A stress model of a hard roof in an automatic roadway formation was established under roof-cutting and unloading conditions. A mechanical analysis was carried out on the deformation of the hard roof during roof cutting and unloading. When the working face was pushed past the cutting seam, the goaf roof was in a state of motion.

(2) Based on a remote ore-pressure monitoring system, surface rock movement, and fracture observation, surface cracks and subsidence were significantly alleviated after roof cutting and pressure relief. Roadway roof movement could be divided into three stages: an active stage of direct roof caving, an active stage of basic roof breaking, and a stable roof stage. Through ore-pressure monitoring, compared with the conventional coal mining area, the affected area of roof-cutting pressure relief increased by 18–22 m, i.e., by approximately twice, a reduction of 20%. It could be known from the observation of drift separation, roof and floor displacement, anchor cable and pillar forced, and shrinkage of live columns. The deformation of the constant resistance anchor cable was less than the subsidence of the roof, which was mainly affected by the bending subsidence of the upper rock layer. However, in the control range of constant resistance anchor cable, the stratum separation value was small, which effectively improved the bearing function of the stratum. The influence range of face propulsion on cable stress was about 30 m and generally ±50 m from the coal of the working face. When the distance of the lagging working face was more than 100 m, the roadway roof separation and roof subsidence tended to be stable, and the maximum shrinkage under active columns was 217 mm. After the pillar was withdrawn for a week, the roof of the roadway tended to be stable. The accumulated subsidence was approximately 9 mm during the period.

(3) A comparison between numerical simulation and actual working conditions showed that the working face pressure at the slotted side of the mining face

was low and that the vertical stress was reduced by approximately 27.5% and the horizontal stress by 24.25%. The influence range of the roadway on the working face's ore pressure was 25 m, and the working face's periodic pressure step distance was 30 m, consistent with the field measured data. After the application of roof-cutting and pressure-relief technology, the stress above the original roadway was gradually transferred to the adjacent working face, forming a stress concentration inside the working face 6 m away from the retained roadway. Nevertheless, the retained roadway was in the stress-reduction zone, thus ensuring the safety of the roadway.

(4) Based on theoretical analysis, field measurement, and numerical simulation, we developed an integral control method for the surrounding rock of the roadway formed by the automatic roof cutting and pressure relief of the 12201 fully mechanized mining face, Halagou Coal Mine. A constant resistance and large deformation anchor cable was added to the side near the cut joint for active support, and a single-hydraulic prop +11# I-steel + steel mesh was used for a combined support at the back of the working face support. A grouting bolt support was used to reinforce the broken loose surrounding rocks at the gangue-retaining side of the tunnel. Through the optimization of the support design, the surrounding rock control effect was found to be remarkable.

Data Availability

The data used to support the findings of this study are included within the article.

Conflicts of Interest

The authors declare no conflicts of interest.

Acknowledgments

This work was supported by Liaoning Provincial Education Department Fund (LJ2017FAL002), Liaoning Innovation and Entrepreneurship Training Plan for College Students (2017101470001), and China Postdoctoral Science Foundation (2020M680490).

References

[1] N. Zhang, C. L. Han, and J. G. Kaniaguang, "The theory and practice of surrounding rock control in retaining roadway along the goaf," *Journal of China Coal Society*, vol. 39, no. 8, pp. 1635–1641, 2014.

[2] Y. Chen, J. B. Bai, and X. Y. Wang, "Research and application of support technology in retaining roadway along goaf," *Journal of China Coal Society*, vol. 37, no. 6, pp. 903–910, 2012.

[3] Q. L. Liu and M. Wang, "The technology of coal pillar less mining in the roadway along the goaf in fully mechanized caving face," *Coal Science and Technology*, vol. 44, no. 5, pp. 122–127, 2016.

[4] X. G. Ma, J. Wang, and H. L. Wu, "Experimental study on topless blasting of coal pillar less mining face in Tashan Coal mine," *Coal Science and Technology*, vol. 46, no. S1, pp. 27–32, 2018.

[5] X. H. Zhang, P. F. Guo, and J. Wang, "Study on optimization experiment of pressure relief borehole spacing along the roadway," *Coal Technology*, vol. 35, no. 6, pp. 6–8, 2016.

[6] Y. J. Wang, M. C. He, and K. X. Zhang, "Characteristics and control measures of mine pressure in mine roadway without coal pillars," *Journal of mining and Safety Engineering*, vol. 35, no. 4, pp. 677–685, 2018.

[7] J. W. Guo and J. W. Zhao, "Study on the breaking rule and control mechanism of the lower roof of the retaining roadway along the goaf," *Journal of mining and Safety Engineering*, vol. 29, no. 6, pp. 802–807, 2012.

[8] S. K. Palei and S. K. Das, "Sensitivity analysis of support safety factor for predicting the effects of contributing parameters on roof falls in underground coal mines," *International Journal of Coal Geology*, vol. 75, no. 4, pp. 241–247, 2008.

[9] M. Lars, "Interaction of shotcrete with rock and rock bolts," *Science Direct*, vol. 45, pp. 538–553, 2007.

[10] J. Hematian, I. Porter, and N. I. Aziz, "Design of roadway support using a strain softening model," in *Proceedings of the 13th International Conference. Ground Control in Mining*, Charlottesville, Virginia, August 1994.

[11] B. G. D. Smart and D. O. Davies, "Application of the rock-title approach to pack design in anArch-sharped roadway," *Mining Engineer*, vol. 12, 1982.

[12] N. G. Baxter, T. P. Watson, and B. N. Whittaker, "A study of the application of T-H support systems in coal mine gate roadways in the UK," *Mining Science and Technology*, vol. 10, no. 2, pp. 167–176, 1990.

[13] G. Williams, "Roof bolting in south wales," *Colliery Guardian*, vol. 11, 2004.

[14] S. Bjurstrom, "Shear strength of hard rock joints reinforced by grouted untensioned bolts," *Proc. of 3rd Congress, ISRM Denver*, vol. II, 1974.

[15] H. H. Sun and B. L. Zhao, *Theory and Practice of Gob Side Entry Retaining*, Coal Industry Press, Pennsylvania, PA, USA, 1993.

[16] H. M. Li, "Design of roof strata control for gob side entry retaining," *Journal of rock mechanics and engineering*, vol. 19, no. 5, pp. 651–654, 2000.

[17] T. Y. Qi, Y. Guo, and C. Hou, "Study on Adaptability of integral pouring roadway protection belt along gob side entry retaining," *Acta Sinica Sinica*, vol. 24, no. 3, pp. 256–260, 1999.

[18] X. Z. Hua, J. F. Ma, and T. J. Xu, "Reinforcement support and parameter optimization of anchor cable beside gob side entry retaining," *Coal Science and Technology*, vol. 32, no. 8, pp. 60–64, 2004.

[19] X. M. Sun and J. Yang, "Study on space-time action law of bolt mesh cable coupling support in deep mining roadway," *Journal of rock mechanics and engineering*, vol. 26, no. 5, pp. 895–897, 2007.

[20] X. M. Fei, "Discussion on the present situation and existing problems of gob side entry retaining support technology in China," *China Science and technology information*, vol. 21, no. 3, pp. 31–33, 2008.

[21] M. C. He and G. Qi, "Deformation failure mechanism and coupling support design of deep composite roof coal roadway," *Journal of rock mechanics and engineering*, vol. 26, no. 5, pp. 988–991, 2007.

[22] X. M. Sun and M. C. He, "Study on nonlinear design method of bolt mesh cable coupling support for deep soft rock

roadway," *Journal of rock mechanics and engineering*, vol. 27, no. 7, pp. 1061–1065, 2006.

[23] X. W. Feng and Z. W. Zhang, "Surrounding rock control technology of rigid flexible secondary coupling support in deep coal roadway," *Mine pressure and roof management*, vol. 4, pp. 18–20, 2001.

[24] F. Peng and X. M. Sun, "Study on the coupling support technology of anchor net and cable in deep coal roadway," *Mine Pressure and Roof Management*, vol. 4, pp. 21–24, 2001.

[25] B. D. Han and C. Y. Peng, "Strata pressure behavior and control of gob side entry retaining," *Coal Science and Technology*, vol. 10, no. 3, pp. 5–8, 2000.

[26] J. X. Liu, P. F. Gou, and Y. S. Zhang, "Analysis of strata pressure behavior in gob side entry retaining," *Ground pressure and roof management*, vol. 7, no. 3, pp. 1–6, 1996.

[27] S. L. Lu, *Ground Pressure Behavior of Roadway Protection without Coal Pillars*, pp. 55-56, Coal Industry Press, Pennsylvania, PA, USA, 1982.

[28] X. M. Guan, L. Lu, and L. S. Zhai, "Study on the law of mine pressure behavior when driving roadway along the goaf in fully mechanized caving face," *Mine pressure and roof management*, vol. 17, pp. 30–33, 2000.

[29] H. M. Li and M. Gu, "Experimental study on gob side entry retaining of No. 9 coal seam in Jincheng mining area," *Journal of Jiaozuo Institute of Technology (NATURAL SCIENCE EDITION)*, vol. 3, pp. 90–93, 2000.

[30] H. H. Sun, J. Wu, and Y. X. Qiu, "Strata behavior and strata control of gob side entry retaining," *Acta coal Sinica*, vol. 1, 1992.

[31] J. Q. Jiang, *Stress and Movement of Stope Surrounding Rock*, Coal Industry Press, Pennsylvania, PA, USA, 1993.

[32] D. Y. Li, *Study on Surrounding Rock Stability of Fully Mechanized Top Coal Caving Face*, Taiyuan University of Technology, Taiyuan, China, 2004.

[33] Q. M. Chen, "Ground pressure behavior characteristics and control technology of gob side entry in fully mechanized top coal caving face," *Acta coal Sinica*, vol. 8, pp. 382–385, 1998.

[34] Y. J. Yang and Y. L. Tan, "Study on the relationship between the deformation affected by mining and the width of coal pillar of roadway protection," *Jiangsu coal*, vol. 3, pp. 9-10, 1995.

[35] D. R. Zhu, *Fracture Law of Main Roof in Longwall Face and its Application*, China University of mining and Technology, Xuzhou, China, 1987.

[36] M. C. He and G. F. Zhang, "Study on the technology of no pillar mining in protective layer of Baijiao Coal Mine by cutting roof along goaf," *Journal of mining and safety engineering*, vol. 21, no. 4, pp. 511–513, 2011.

[37] H. Liu, "Study on the technology of automatic coal roadway without coal pillars in large depth and medium thick seam of Chengjiao Coal mine," *Energy and Environment Protection*, vol. 40, no. 11, pp. 193–198, 2018.

[38] H. H. Yang, E. L. Xue, and W. Luo, "Application of Shenhua Group's top-loading pressure relief automatic roadway without coal pillar mining technology," *Coal Science and Technology*, vol. 3, pp. 1–3, 2015.

[39] M. C. He, W. F. Cao, and R. L. Shang, "A new technology of two-dimensional shaped energy stretch blasting," *Chinese Journal of Rock Mechanics and Engineering*, vol. 12, pp. 2047–2051, 2003.

[40] M. C. He, Y. B. Gao, and J. Yang, "Experimental study on self-forming tunnel of quick-recovery and top-loading unloading and non-coal pillar in thick coal seam," *Rock and Soil Mechanics*, vol. 39, no. 1, pp. 254–264, 2018.

[41] Y. B. Gao, J. Yang, and M. C. He, "Study on deformation mechanism and control technology of gravel gangway without coal pillar cutting in thick coal seam," *Chinese Journal of Rock Mechanics and Engineering*, vol. 36, no. 10, pp. 2492–2502, 2017.

[42] G. F. Zhang, M. C. He, and X. P. Yu, "Study on mining technology of non-coal pillars along the goaf of Baijimine protection layer," *Journal of mining and Safety Engineering*, vol. 28, no. 4, pp. 511–516, 2011.

[43] E. L. Xue, Z. H. Ma, and W. Luo, "Study on the mining pressure law of automatic roadway with shallow top-buried composite roof under pressure relief," *Coal Science and Technology*, vol. 2017, no. s1, pp. 34–38, 2017.

[44] K. Wang, T. H. Kang, and H. T. Li, "Study on the method of controlling roof placement and reasonable suspension length of hard roof," *Chinese Journal of Rock Mechanics and Engineering*, vol. 28, no. 11, pp. 2320–2327, 2009.

[45] Z. H. Chen, J. J. Feng, and C. C. Xiao, "Mechanical model of roof fracture in fully mechanized top coal caving mining in shallow deep seam," *Journal of China Coal Society*, vol. 32, no. 5, pp. 449–452, 2007.

[46] P. F. Guo, G. F. Zhang, and Z. G. Tao, "Blasting technology of roadway retaining in hard and weak composite roof with top pressure relief," *Coal Science and Technology*, vol. 44, no. 10, pp. 120–124, 2016.

[47] Z. B. Guo, J. Wang, and T. P. Cao, "Study on key parameters of automatic roadway of thin coal seam cutting and pressure relieving," *Journal of China University of Mining and Technology*, vol. 45, no. 5, pp. 879–885, 2016.